

First Hybrid Turbulence Modeling for Turbine Blade Cooling

Sagar Kapadia^{*} and Subrata Roy[†]

*Computational Plasma Dynamics Laboratory
Kettering University
Flint, Michigan 48504, USA*

James Heidmann[‡]

*Turbomachinery and Propulsion Systems Division
NASA Glenn Research Center, Cleveland, Ohio USA*

INTRODUCTION

Gas turbines require proper cooling mechanism to protect the airfoils from thermal stresses generated by exposure to hot combustion gases. The problem becomes aggravated by the growing trend to use higher turbine inlet temperature to generate more power. Thus, film cooling is used as a cooling mechanism and it works in the form of row of holes located in the spanwise direction, through which cold jets are issued into the hot crossflow. The penetration of cold jet into the main flow creates a complex flowfield. Systematic investigation of such flowfield started in late 50s. Figure 1 shows the schematic of a single round jet injected in the crossflow at an angle $\alpha=35^\circ$. Figure also describes the boundary conditions applied at different faces. Even though use of symmetry boundary condition at the hole centerline would reduce the computational time by half, its use is avoided as it prevents the possibility of capturing the unsteady asymmetric vortical flow patterns. This geometry is well accepted for the gas turbine community and has been extensively

^{*} Graduate Research Assistant, Email: kapa9202@kettering.edu, AIAA Student member.

[†] Associate Professor and Director, Email: sroy@kettering.edu, AIAA Associate Fellow

[‡] Research Engineer, Email: james.heidmann@grc.nasa.gov, AIAA Member

studied¹ for cooling performance for a wide range of blowing ratios, $M = \rho_j V_j / \rho_{fs} V_{fs}$, where ρ and V are density and normal velocity, respectively for jet (j) and freestream (fs).

Goldstein² correlated film cooling effectiveness $\eta = (T_{fs} - T) / (T_{fs} - T_j)$ with the parameter x/Mb , where x is the downstream distance, M is the blowing ratio, b is the slot width and T_{fs} , T and T_j are the temperatures of crossflow, blade and jet respectively. Sinha et al.¹ carried out experimental work to study the relationship between the fluid-thermal parameters of jet and film cooling effectiveness using a row of inclined holes.

The mixing of a jet in a cross-stream is a fully three-dimensional phenomenon³. Amer et al.⁴ pointed out that the flow predictions are greatly affected by the selection of the turbulence model. Roy⁵ documented the cooling performance of twelve different arrangements of holes with a combination of blowing ratio M , distance between the holes L and jet angle α using a upwind biased finite volume code and standard $k-\omega$ turbulence closure model. Garg and Rigby⁶ resolved the plenum and hole pipes for a three-row showerhead film cooling arrangement with Wilcox's $k-\omega$ turbulence model. Heidmann et al.⁷ used RaNS to compute the heat transfer for a realistic turbine vane with 12 rows of film cooling holes with shaped holes and plena resolved. Though these studies provide good details of the flow, the anisotropic dynamic nature of the spanwise vortices that affect the film cooling process are more complex than that can be captured by the mixing models used in aforementioned papers. Acharya⁸ compared the results of $k-\varepsilon$ and RST (Reynolds Stress Transport) turbulence models with the data of direct numerical simulation (DNS) and large eddy simulation (LES) for a film cooling problem and concluded that as compared to DNS and LES two-equation RaNS models generally underpredict the lateral spreading of the jet and overpredict the penetration due to an assumption of isotropic eddy viscosity. Though direct numerical simulation (DNS) and large eddy simulation (LES) can capture minor flow details, these methods are

computationally limited for high Reynolds number flows. For $Re = 4700$, the LES solution on $122 \times 52 \times 32$ node mesh took 1-2 days in Digital Alpha 500 workstation. As a viable alternative, this paper presents the *first* detached eddy simulation (DES) based hybrid modeling of film cooling flow for the three-dimensional geometry in Figure 1. The result is also compared with the values of centerline and spanwise effectiveness with the experiment values obtained by Sinha et al.¹

Hybrid Turbulence model

The two competing factors important for any turbulence model are accuracy and efficiency (i.e. computational cost). Proposed by Spalart et al.⁹, DES is a hybrid model which combines the efficiency of RANS and the accuracy of LES length scales to work under a single framework. DES works by applying a variable length scale that varies as a function of the distance to the nearest wall (d_w) in the attached boundary layer and conforms with sub-grid scale in the rest of the flow including separated regions and near wake¹⁰. Two different DES models^{10,11} are currently available in the numerical code¹² used in the present simulation:

- (1) S-A (Spalart-Allmaras) based DES model,
- (2) M-SST (Menter's shear stress transport) based DES model.

Spalart-Allmaras¹³ based DES model is used in the present study. S-A is a one equation RANS model. A detailed information about S-A one equation model, which is used in the presented DES simulation is given by Squires et al.¹¹.

Spalart-Allmaras based DES model has been developed in such a way that the model works as S-A RANS model near the wall surfaces and acts as a subgrid LES model away from the wall. In S-A based DES formulation, distance to the nearest wall, d_w is replaced by \tilde{d} , where \tilde{d} is defined as,

$$\tilde{d} = \min(d_w, C_{DES}\Delta) \quad (1)$$

where, C_{DES} is a model constant and for S-A based DES model, $C_{DES}=0.65$ and Δ is the largest distance between the cell center under consideration and the cell center of the neighbors. The model works as a standard S-A turbulence model inside the numerically predicted boundary layer. In the regions, far from the wall, where $d_w > C_{DES}\Delta$, the length scale becomes grid-dependent and the model performs as a subgrid-scale version of the S-A model for eddy viscosity. When production and destruction terms balance each other, this model reduces to an algebraic mixing-length Smagorinski-like subgrid model. Recently, Kapadia et al.¹⁴ have successfully implemented DES for external flow analysis over a ground vehicle.

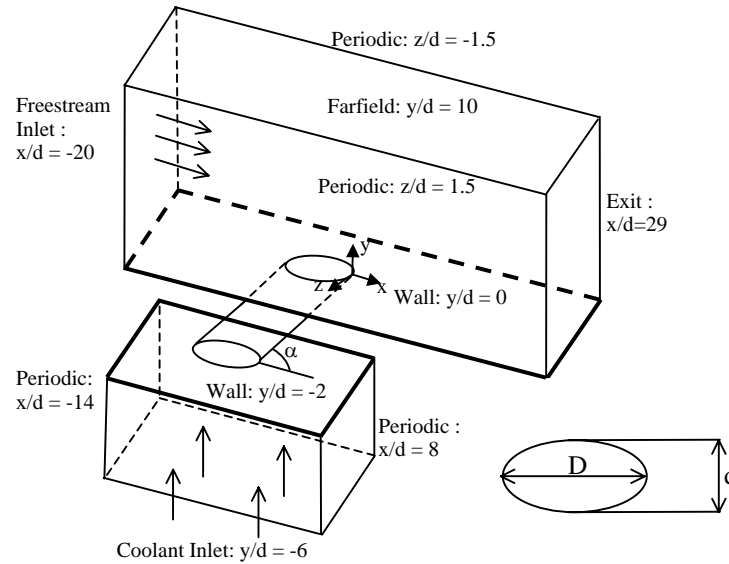


Figure 1. Schematic of the film cooling flow. Actual geometry definition and boundary conditions are based on Sinha et al¹.

Grid information and Computational approach

Present study implements Cobalt¹², a parallel, implicit, unstructured finite-volume based flow solver that uses second-order accurate spatial and temporal Godunov schemes.¹⁵ A multi-block computational grid was initially developed using the GridPro multiples grid generator with 15 blocks and approximately 2,600,000 computational cells. Gridgen14.03 is used to convert this grid into

Cobalt compatible unstructured grid. The final grid used in the solution contains single block and 2,109,440 cells which is approximately 10 times denser than Acharya's mesh.⁸ The Reynolds number based on the diameter and inlet conditions at the hole was 19700. Viscous clustering was employed at all solid walls with a y^+ value less than 1.0 at all locations. Stretching ratios less than 1.2 were used normal to the viscous walls. Iteration convergence was considered achieved when all residuals reduce by four orders of magnitude. Size of the time-step is a function of CFL, which increases from 10^3 to 10^6 during initial 130 time-steps and remains constant for the remaining time-steps, yielding the maximum time-step size of 6.17×10^{-4} sec. Present case is run on the cluster of 64 parallel processors on Blue Horizon supercomputer at SDSC. The aggregate CPU time requirement for the entire DES solution is 37.46 seconds/iteration and that for one cell is 17.76 micro seconds/iteration. Total CPU requirement for the solution to complete 6000 time-steps (real time 3.7sec) is approximately 4000 hours. Extrapolating, it is easy to estimate that for a coarser mesh⁸ DES solution will take less than 16 hrs. As size of the time-step is not very small in the present case, simulation was run using two Newton sub-iterations to reduce linearization errors in the Jacobian. This increased the computational time by three times than normal iteration (without Newton sub-iteration, which is common for a steady state solution).

RESULTS AND DISCUSSION

Figure 1 describes schematic control volume, in which hot air at 300K passes over a flat surface and cool air at 150K is issued at an angle $\alpha=35^\circ$. The intersection of the injection pipe with the wind tunnel forms an ellipse with the minor and the major axes of $d=2.54\text{mm}$ and $D=d/(\sin\alpha)$, respectively. The presented numerical simulation uses blowing ratio of 1, density ratio of 2 and velocity ratio of 0.5. Fixed mass flow rate and stagnation temperature inlet boundary conditions are employed for the plenum and freestream. Fixed static pressure boundary condition is applied at the

exit. Adiabatic no-slip conditions are applied at all solid walls, including the inner surface of the film hole and the plenum. A maximum Mach number not exceeding 0.3 was achieved in the flow field while maintaining the desired Reynolds number by scaling the experimental geometry¹ down by a factor of 5. Figures 2-6 described in this section correspond to the time-averaged DES solution after 3.7 sec, when solution reaches at quasi-stationary state.

Figure 2 shows velocity vectors highlighted by the magnitude of streamwise velocity at the hole centerline ($z = 0$). It also shows the interface between RaNS and LES region, where $d_w = C_{des} \Delta$. It is evident from the figure that the treatment of the initial penetration of jet into freestream is carried out by pure LES technique. This is due to the fine spanwise spacing at the hole exit which switches the code to LES mode.

Figure 3 shows two iso-surfaces of z-vorticity stratified by temperature. The values of the z-vorticity for the left and right iso-surfaces are -10000 s^{-1} and $+10000 \text{ s}^{-1}$ respectively. Light and dark shades of greyscales represent 300 K and 150K respectively. The injection pipe is shown as reference. It is evident that maximum recirculation is present at the location of initial interaction between the jet and crossflow. The recirculation near the wake region follows a pair of counter-rotating vortices. A sharp temperature gradient is present near the trailing edge of the hole, which becomes more diffused as the flow progresses downstream.

The normalized wall temperature distribution in Figure 4 indicates that the minimum temperature (0.5) exists at the hole. Downstream maximum cooling takes place in a small area just beyond (less than 1d) the trailing edge of the hole where the normalized wall temperature is 0.73. In the streamwise direction beginning at approximately 6d, the normalized temperature reduces to 0.78 and remains cool for nearly 7d.

Film cooling is a strongly coupled fluid-thermal process. Figure 5 plots the effect of flow structures on normalized fluid temperature on a vertical plane at $x=3.5d$. Presence of asymmetry is

present in the unsteady solution for both velocity vectors and temperature profile. Time-averaged data shows prominent features of elongated kidney-shaped bound vortices followed by similar temperature profiles.

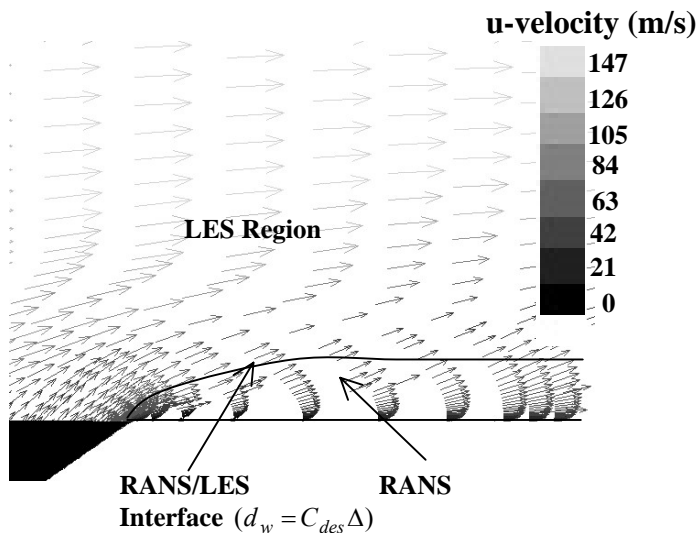


Figure 2. DES/RaNS interface and velocity vectors highlighted by u-velocity at hole centerline.

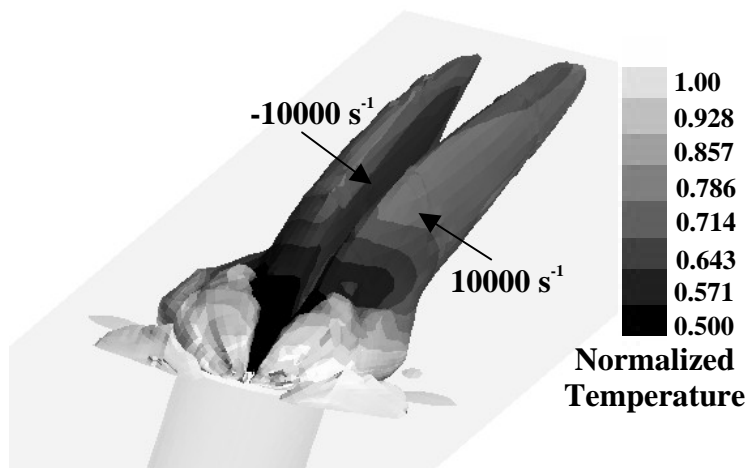


Figure 3. Two Iso-surfaces of x-vorticity (-10K and 10K) stratified by the temperature.

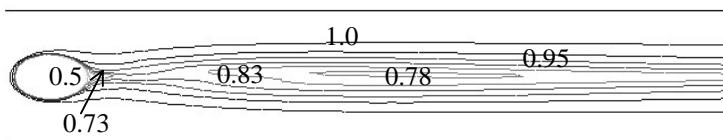


Figure 4. Temperature contours normalized by the freestream temperature.

Comparison between experimental¹ and numerical (time-averaged DES) values of the centerline and the span-averaged effectiveness is done in Figures 6 (a) and (b) respectively. The sharp difference between the experimental¹ and DES time-averaged results for centerline effectiveness at $x = 1d$ stems from the fact that although numerical prediction of maximum cooling occurs near the trailing edge of the hole (similar to the experimental data), its spanwise distribution is very narrow, less than $1d$ (Figure 4). The experimental and numerical effectiveness follow similar trend between $x=1d$ to $x = 6d$. Beyond $6d$, numerical centerline effectiveness shows higher value than the experimental data, while numerical span-averaged effectiveness is lower in that region. Figure 4 clearly shows that there is very little diffusion in the spanwise direction for DES results, which is responsible for the small values of span-averaged effectiveness.

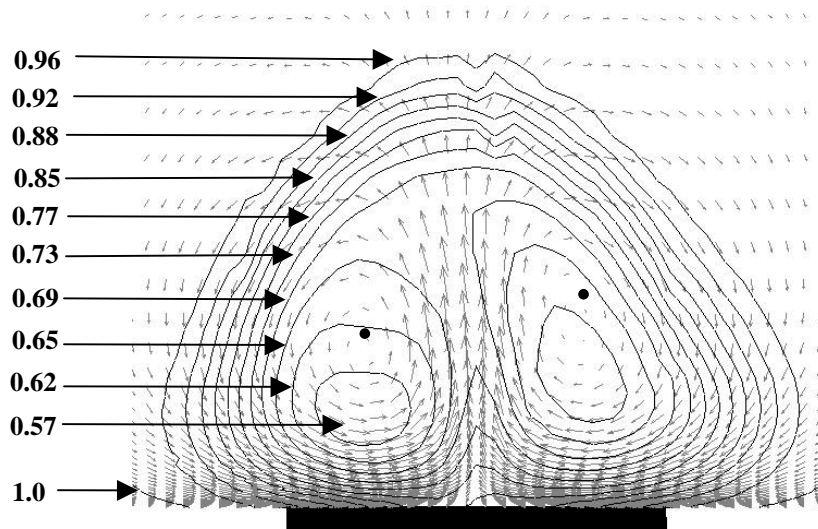


Figure 5. Velocity vectors with superimposed normalized temperature contours at $x/d = 3.5$ for time-averaged DES solution.

Conclusions

The first detached eddy simulation of film cooling has been presented for a widely published plate-pipe configuration. The blowing ratio was unity and density ratio was two. Results indicate that the mixing processes downstream of the hole are highly anisotropic. DES solution shows its ability

to depict the dynamic nature of the flow and capture the asymmetry present in temperature and velocity distributions. Further, comparison between experimental and DES time-averaged effectiveness is satisfactory. Numerical values of centerline and span-averaged effectiveness differ from that of experimental values at downstream locations. Smaller values of numerically predicted spanwise effectiveness than the experimental data may be due to the improper turbulence model in the spanwise spreading of the jet. This needs to be investigated in the near future.

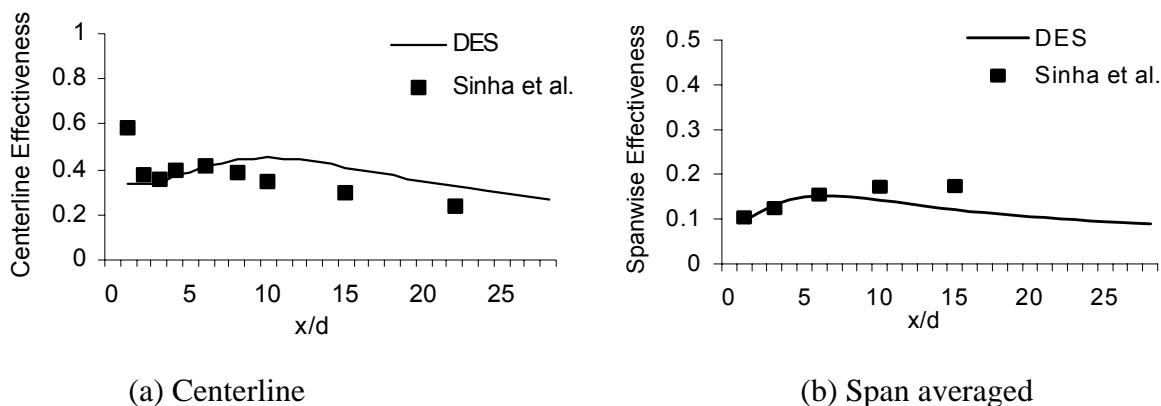


Figure 6. Comparison between experimental and numerical effectiveness.

References

- ¹Sinha, A. K., Bogard, D. G., and Crawford, M. E., "Film-Cooling Effectiveness Downstream of a Single Row of Holes With Variable Density Ratio," *Journal of Turbomachinery*, Vol. 113, 1991, pp. 442-449.
- ²Goldstein, R. J., "Film Cooling, *Advances in Heat Transfer*", Vol. 7, Academic press, New York, 1971, pp. 321-379.
- ³Fric, T. F., and Rosko, A., "Vortical structure in the wake of a transverse jet," *Journal of Fluid Mechanics*, Vol. 279, 1994, pp. 1-47.
- ⁴Amer, B., Jubran, A., and Hamdan, M. A., "Comparison of different two-equation turbulence models for prediction of film cooling from two rows of holes," *Journal of Numerical Heat Transfer, Part A*, Vol. 21, No. 2, 1992, pp. 143-163.

⁵Roy, S., "Numerical Investigation of the Blade Cooling Effect by Multiple Jets Issuing at an angle," Journal of Numerical Heat Transfer, Vol. 38, No. 7, 2000, pp. 701-718.

⁶Garg, V. K., and Rigby, D. L., "Heat Transfer on a Film-Cooled Blade - Effect of Hole Physics," International Journal of Heat and Fluid Flow, Vol. 20, 1999, pp.10-25.

⁷Heidmann, J. D., Rigby, D. L., and Ameri, A. A., "A Three-Dimensional Coupled Internal/External Simulation of a Film-Cooled Turbine Vane," Journal of Turbomachinery, 122, 2000, pp. 348-359.

⁸Acharya, S., "Large Eddy Simulations and Turbulence Modeling for Film Cooling," NASA/CR – 1999-209310, pp. 1-131.

⁹Spalart, P. R., Jou W. H., Strelets, M., and Allmaras, S. R., "Comments on the Feasibility of LES for Wings, and on a Hybrid RANS/LES Approach," First AFOSR International Conference on DNS/LES, Ruston, Louisiana, 1997.

¹⁰Strelets, M., "Detached Eddy Simulation of Massively Separated Flows," AIAA Paper 01-0879, Jan. 2001.

¹¹Squires, K. D., Forsythe, J. R., Morton, S. A., Strang, W. Z., Wurtzler, K. E., Tomaro, R. F., Grismer, M. J., and Spalart, P. R., "Progress on Detached-Eddy Simulation of Massively Separated Flows," AIAA Paper 02-1021, Jan. 2002.

¹²Grismer, M. J., Strang, W. Z., Tomaro, R. F., and Witzeman, F. C., "Cobalt: A parallel, implicit, unstructured Euler/Navier-Stokes solver," Adv. Engg. Software, Vol. 29, No. 3-6, 1998, pp.365-373.

¹³Spalart, P. R., and Allmaras, S. R., "A One-Equation Turbulence Model for Aerodynamic Flows," AIAA Paper 92-0439, Jan. 1992.

¹⁴Kapadia, S., Roy, S., and Wurtzler, K., "Detached Eddy Simulation Over a Reference Ahmed Car Model," AIAA Paper 03-0857, Jan. 2003.

¹⁵Godunov, S. K., "A difference scheme for numerical computation of discontinuous solution of hydrodynamic equations," Journal of Computational Physics, Vol. 32, 1979, pp.101-136.